Electrostatic Core Shielding in Dendritic Polyglutamic Porphyrins

Sergei A. Vinogradov* and David F. Wilson[a]

Abstract: Polyglutamic dendritic porphyrins of the general formula H_2Poph-Glu^{N}OR (H_2Porph = free-base *meso*-tetra-4-carboxyphenylporphyrin (H_2TCPP), Glu = dendrimer layer composed of L-glutamates, $N = 1-3$: dendrimer generation number, R = terminal group (All, H)) were synthesized and characterized with NMR and MALDI-TOF mass spectroscopy. The free-acid terminated compounds were found to be highly soluble in water, with both their absorption and fluorescence spectra dependent on pH. The value of the porphyrin mono-protonation constant, measured by fluorescence rationing, increased monotonously in the studied series of dendrimers ($pK_3 = 6.31$, 6.70, and 6.98, for $N = 1$, 2, 3, respectively). For the largest dendrimer, H_2PorphGlu^{3}OH, pK_3 was found shifted by almost two pH units relative to the non-modified H_2Porph. The second protonation constant (K_4) was much less affected by the dendritic substituents. At pH values less than 3.5 there were noticeable changes in fluorescence intensity and quantum yield even for the highly soluble H_2PorphGlu^{3}OH. This suggests that interactions between individual dendritic molecules in solution are favored by full protonation of the peripheral glutamic carboxyls. The "dendrimer-protected" porphyrins are convenient fluorescent pH sensors in the biological pH range.

Keywords: dendrimers · fluorescence · porphyrinoids · protonations · UV/Vis spectroscopy

Introduction

There has been a substantial body of work reported over the past decade on so called "functional dendrimers".[1] These are dendritic polymers carrying a fragment designed to perform a range of specific functions, such as absorbing light and passing energy and/or a charge onto another molecule, catalyzing a chemical transformation, or forming a complex with a chosen ligand. Dendrimers with porphyrin cores[2–10] make up an important group of functional dendrimers. These are interesting because of their close structural and functional relationship with heme containing proteins,[3, 4] their enhanced catalytic selectivity,[5] unusual interactions with other molecules[6] and outstanding electro- and photochemical properties.[7, 8] In addition, due to the unique control, which dendrimers provide over the porphyrin microenvironment, dendrimer–porphyrins have one more area of use, namely the optical probing of small molecules.

Recently, we reported a series of dendritic polyglutamic Pd–porphyrins, designed for O_2 sensing by phosphorescence quenching.[10] The shielding effect of the dendritic cages, monitored through the interactions of the triplet state porphyrins with O_2, was found to be dependent on solvent polarity. Our interpretation of the phenomenon involved solvent-dependent conformational changes in the dendrimer body. In addition to the dendrimer conformation per se, the properties of the core itself and/or its accessibility to the quencher can also be influenced by the peripheral charge on the dendrimer. Electrostatic shielding has been previously demonstrated by cyclic voltammetry in Zn and Fe polyether amide dendrimer–porphyrins.[4a,c] It also has been shown that interactions between a negatively charged surface and a positively charged quencher of relatively large size (e.g., methylviologen di-cation) facilitated fluorescence quenching in the series of Zn polyarylether dendritic porphyrins, presumably through dendrimer conducted electron transfer.[7a] The recent photo-physical data for the series of dendritic $[Ru(bpy)_3]^{2+}$ complexes also confirmed that quenching patterns are strongly dependent on the charge of the quencher and the surface charge of the dendritic shell.[11]

To investigate the effect of a peripheral charge on the central core moiety, we studied the N-protonation of free-base porphyrins, encapsulated inside polyglutamic dendrimers of three different sizes, and consequently surrounded by different amounts of negatively charged carboxyls. Both absorption and fluorescent spectra of free-base porphyrins change significantly upon imine N-protonation.[12] Herein we report pH titrations in the series of dendritic polyglutamic porphyrins, as measured by absorption and fluorescence spectroscopy.

[a] Dr. S. A. Vinogradov, Prof. D. F. Wilson
Department of Biochemistry and Biophysics
School of Medicine, University of Pennsylvania
Philadelphia, PA 19104 (USA)
Fax: (+1) 215-573-3787
E-mail: vinograd@mail.med.upenn.edu

Supporting information for this contribution is available on the WWW under http://www.wiley-vch.de/home/chemistry/

  0947-6539/00/0613-2456 $ 17.50+.50/0

Experimental Section

The synthesis of all the dendrimers described in this paper has been exactly the same as in our previous work,[10b] excepting only the use of free-base *meso*-tetra-4-carboxyphenylporphyrin (H_2TCPP) as an initiator-core instead of its Pd-complex. Thus, all the materials and methods are identical to those used in ref.[10b] H_2TCPP was prepared by hydrolysis (NaOH/aqueous methanol) of the corresponding tetramethyl ester, *meso*-tetra-4-methylcarboxyphenylporphyrin (H_2TMCPP). The latter was synthesized by the standard condensation of pyrrole (Aldrich) with terephthalaldehydic acid methyl ester (TCI America), following the previously published method[13] (also see[10b] for details).

All the instrumentation used in this work has been described in detail elsewhere.[10b] UV/Vis absorption spectra and fluorescence spectra were recorded on Beckman DU-64 spectrophotometer and on SPF-500C spectrofluorometer (SLM Instruments, Inc., USA). To obtain a series of samples for spectrophotometric pH titration a small amount of the material (dendritic porphyrin) was dissolved in 50 mM Na_2HPO_4 solution (300 mL) at pH ≈ 11. The absorbance of the solution (1 cm cuvette) at a maximum of the Soret band was kept at <0.4. Thus, absorbance in the region of $\alpha-\delta$ bands was always below 0.05. The small aliquots (≈2–3 mL) of solution with the pH adjusted by addition of conc. aq. HCl were stored in glass tubes. The same sets of samples were used for the measurements of both absorption and fluorescence.

The fluorescence quantum yields were obtained by comparing the integrals of the corrected emission spectra with those of free-base *meso*-tetraphenylporphyrin (H_2TPP) in benzene. The spectra were normalized by the optical density of the samples at the excitation wavelength, relative photon intensity of the source and quantum efficiency of the detector (Hamamatsu R928 PMT) throughout the entire emission range. The reported quantum yield value for H_2TPP in C_6H_6 is 11%.[14]

Results and Discussion

Synthesis of dendrimers with the general formula H_2PorphGlu^{N}OR, where H_2Porph = H_2-*meso*-tetra-4-carboxyphenylporphyrin (H_2TCPP), Glu = dendrimer layer composed of L-glutamates, $N = 1-3$: dendrimer generation number, and R = allyl, H: terminal group, was performed according to the scheme previously employed in the synthesis of the corresponding Pd-complexes.[10b] All allyl-esters (**1a**, **2a**, and **3a**) were purified using chromatography on silica gel. The acid-terminated porphyrin–dendrimers changed to a deep green upon acidification of water solutions. While H_2PorphGlu^{1}OH (**1**) and H_2PorphGlu^{2}OH (**2**) were collected by precipitation and subsequent filtration, dendrimer H_2PorphGlu^{3}H (**3**) had to be dialyzed against distilled water and isolated by freeze drying because of its almost unlimited solubility in water even under highly acidic conditions.

The structural formulas of the synthesized dendrimer–porphyrins are shown on Figure 1. The structures were confirmed by ^{1}H-, ^{13}C-NMR, and MALDI-TOF mass spectroscopy. Both NMR and mass spectra are very similar to those of Pd-complexes. The latter were discussed in detail elsewhere.[10b]

Absorption spectroscopy: The absorption spectroscopy data are summarized in Table 1. It has been shown previously that in the series of polyarylether dendritic Zn-porphyrins the Soret absorption maximum becomes progressively red-shifted with an increase in dendrimer size.[7a] Similarly, small (≈1.5 nm) but reproducible shifts were detected in the series H_2PorphGlu^{N}OR ($N = 1-3$) in both H_2O and organic solvents

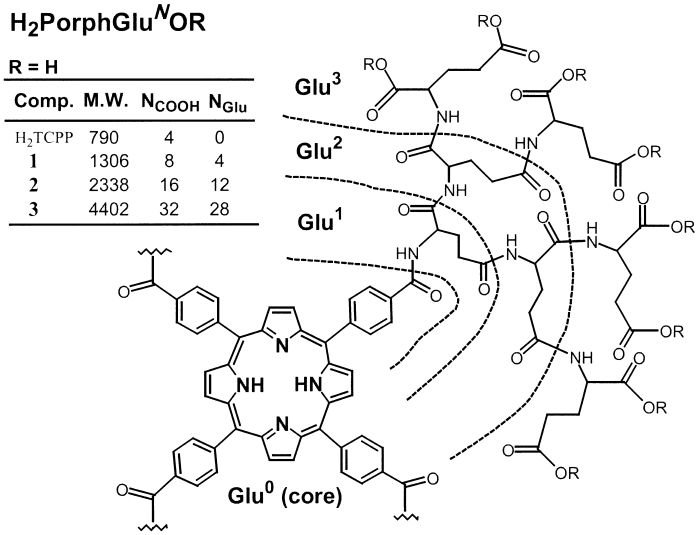

Figure 1. Structural formulae of the synthesized dendrimer–porphyrins. The same polyglutamic dendrons are attached to all four phenyl rings of the core-porphyrin. The table shows molecular weights, number of the terminal carboxyl groups, and total number of glutamates per molecule.

Table 1. Absorption data of H_2PorphGlu^{N}OR.

Generation	R	Solvent	Soret (λ, nm)	Visible bands (λ, nm)
	Me	CH_2Cl_2	418	514.5, 547, 590, 647.5
N **= 0**	Me	DMF	418	513, 547, 591, 647
	OH	DMF	418	514, 548, 591, 647
	OH	H_2O	414	515, 553, 580, 634
	OH	H_2O/TFA	469[a]	–
	All	CH_2Cl_2	418	515, 547.5, 591.5, 647
N **= 1**	All	DMF	418	514, 547, 591, 647
	OH	DMF	418	513.5, 547, 590, 647
	OH	H_2O	414	515.5, 553, 580, 635
	OH	H_2O/HCl	435; 453[b]	648, 664,[b] 695[b]
	All	CH_2Cl_2	418.5	515, 548, 592, 647
N **= 2**	All	DMF	418.5	514, 547, 591, 647
	OH	DMF	419	514, 548, 591, 647
	OH	H_2O	414.5	516, 553, 580, 637
	OH	H_2O/HCl	436.5, 460[c]	650, 664[b]
	All	CH_2Cl_2	419.5	515.5, 550, 592, 647.5
N **= 3**	All	DMF	419.5	515, 548, 590, 648
	OH	H_2O	415.5	516, 554, 583, 637
	OH	H_2O/HCl	438, 441[d]	650, 657[d]

[a] Ref. [17b]. [b] Assigned to the aggregates formed upon acidification. [c] "Shoulder" with approximate position of the maximum. [d] Hypothetical assemblies between the dendrimers.

(CH_2Cl_2 and DMF); this indicates a rather open architecture of the dendritic branches. In these dendrimers the branches were attached to the *para*-positions of *meso*-phenyl substituents on the porphyrin. For this type of substitution in polyarylether dendrimers the architecture was still considered "semiclosed" even for the higher generations ($N = 5$).[6a]

To demonstrate how the increasing size of a polyglutamic dendrimer alters the properties of the encapsulated porphyrin we studied the pH dependence of the absorption spectra in the H_2PorphGlu^{N}OH series. Upon addition of acid, the spectra of *meso*-phenyl substituted porphyrins obtain a typical "two" Q-band pattern, consistent with the increase in molecular symmetry up to D_{4h} in di-protonated form (Scheme 1).[15, 16]

$$\left[(\text{PorphGlu}^{N}\text{OH})^{2-} \underset{-H^+}{\overset{K_1}{\rightleftharpoons}} (\text{HPorphGlu}^{N}\text{OH})^{-}\right] \underset{-H^+}{\overset{K_2}{\rightleftharpoons}}$$

$$\rightleftharpoons \text{H}_2\text{PorphGlu}^{N}\text{OH} \underset{+H^+}{\overset{K_3}{\rightleftharpoons}} (\text{H}_3\text{PorphGlu}^{N}\text{OH})^{+} \underset{+H^+}{\overset{K_4}{\rightleftharpoons}} (\text{H}_4\text{PorphGlu}^{N}\text{OH})^{2+}$$

Scheme 1.

The Soret peaks of di-protonated porphyrins are shifted about 30 nm to the red. For porphyrins with negatively charged groups on the periphery, such as *meso-para*-tetrasulfonatophenyl porphyrin (H_2TSPP) or H_2TCPP, a further red shift occurs with higher acidity, which has been attributed to the formation of the stabilized intermolecular aggregates (see, for example, ref.[17, 18] and references therein).

In the H_2PorphGlu^{N}OH ($N=1-3$) series, N-protonation caused similar spectral changes, however, these occurred at different pH values, depending on the dendrimer size. Selected absorption spectra of H_2PorphGlu^{N}OH are shown in Figure 2.

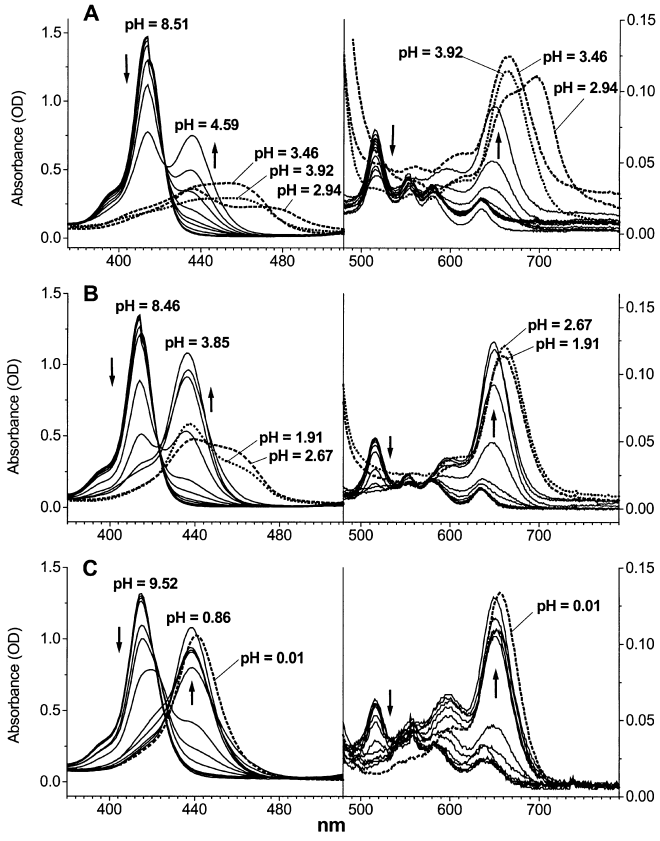

Figure 2. Changes in the electronic absorption spectra in H_2PorphGlu^N-OH-series of dendrimers, induced by N-protonation. Arrows (shown above the corresponding Soret peaks) indicate the directions of the spectral changes upon gradual acidification, from maximal to minimal pH values. Dashed lines show the spectra of the intermolecular aggregates. A) H_2PorphGlu^{1}OH ($N=1$) (**1**). B) H_2PorphGlu^{2}OH ($N=2$) (**2**). C) H_2PorphGlu^{3}OH ($N=3$) (**3**).

N-protonation bathochromically shifts Soret bands of all the studied dendrimer–porphyrins. Confirmed by the florescence data (vide infra), formation of the porphyrin monocations is complete before water solubility becomes low enough to cause aggregation. This holds true even for the smallest, least soluble dendrimer H_2PorphGlu^{1}OH (**1**). Aggregation of compound **1** starts at a critical pH 4.6–4.7 (Figure 2, A), whereas a significant peak at 435 nm, which is due to its di-protonated form $(H_4\text{PorphGlu}^1\text{OH})^{2+}$, is readily seen by pH 4.0. At pH 4.59 this band reaches maximal intensity, but even at maximum it is only half the size of the peak at 414 nm ($r_{435/414}=0.5$), originated from the non-protonated form. The critical pH value of the H_2PorphGlu^{2}OH (**2**) aggregation is lower, 3.0–3.2 (Figure 2, B), and more of the di-protonated but not yet aggregated porphyrin remains in solution ($r_{435/414}=0.85$). It is seen from Figure 2 that for the generation 3 dendrimer, H_2PorphGlu^{3}OH (**3**), intermolecular interactions do not affect the absorption spectra until pH is very acidic (pH $\approx$ 0.01).

Notably, the difference between Soret maxima of the smallest ($N=1$) and the largest ($N=3$) dendrimers in the series is bigger for the protonated forms $(H_4\text{PorphGlu}^N\text{OH})^{2+}$ ($\lambda_{\text{Soret}}{}^{N=3}-\lambda_{\text{Soret}}{}^{N=1}\approx 2.5$ nm) than for the non-protonated ones ($\lambda_{\text{Soret}}{}^{N=3}-\lambda_{\text{Soret}}{}^{N=1}\approx 1.5$ nm). Assuming that such differences are due to alterations in the porphyrin microenvironment, this suggests that at a lower pH, dendrimers form more dense structures around the core. A formed hydrophobic matrix offers stronger "protection" to the porphyrin. The corresponding pH dependence was observed for O_2 quenching rates of PdPorphGlu^{3}OH in H_2O.[10]

Our experiments were carried out in buffered water solutions, with pH gradually adjusted by the addition of HCl. Upon increasing acidification, solutions of **1** and **2** eventually became opalescent and then precipitation occurred. There was also a noticeable decrease in the fluorescence intensity (vide infra) of the acidic samples; this suggests formation of intermolecular aggregates. Prior to precipitation, the acidification of both **1** and **2** caused the appearance of red-shifted bands, very similar to those described previously for the aggregated $H_4{}^{2+}$TCPP.[17b] These bands were attributed to the J-type aggregates, common to the protonated *meso*-tetraarylporphyrins, for example $H_4{}^{2+}$TCPP, $H_4{}^{2+}$TSPP, and to other porphyrins as well.[19] However, in our case the porphyrins with one or two dendritic glutamic layers were less likely to form such structures due to the simple steric considerations.

The longer wavelength bands at 460 and 664 nm were not found in the spectra of the generation 3 dendrimer, H_2PorphGlu^{3}OH (**3**). This compound remained soluble throughout the entire pH range, and it was possible to titrate its solutions to very acidic pH values (pH $\approx$ 0.01). It is under such extremely acidic conditions that the red-shifted Soret and Q-bands were observed in the spectra of $H_4{}^{2+}$TCPP (in 10 vol.% of CF_3COOH).[17b] Upon acidification of **3** (pH $\approx$ 0.01) the Soret peak (438.5 nm) shifted to the red ($\approx$442 nm), and an even larger shift, from 650 nm to 657 nm, was observed in the Q-band (Figure 2, C). The J-type porphyrin aggregation is impossible in the case of dendrimer **3**. Thus, bathochromic shifts as well as the decreased fluorescence intensity (vide infra) must be due to some longer-range interactions between the porphyrin chromophors. Such interactions through the dendrimer network have been previously proposed in the literature.[7a] Under highly acidic conditions all peripheral carboxyls of polyglutamates are protonated.[20a] The lack of

0947-6539/00/0613-2458 $ 17.50+.50/0 *Chem. Eur. J.* **2000**, *6*, No. 13

repulsion between the negative charges allows the polyglutamic branches to fold into a denser structure around the porphyrin, and also favors formation of intermolecular assemblies between the dendrimers. As a result, at acidic pHs the actual distance between porphyrins in aggregates becomes shorter and the dendrimer separating them becomes more dense and consequently more conductive. Both factors could lead to an increased self-quenching of fluorescence.

Fluorescence spectroscopy: The fluorescence spectra of $H_2PorphGlu^NOH$ ($N=1$, 2) are shown in Figure 3, and the corresponding positions of the emission maxima are summarized in Table 2. The same sets of samples were used for both absorption and fluorescence measurements. In order to avoid signal saturation due to the excessive absorption of the excitation light, the excitation was carried out at 485 nm, a region well separated from both Soret peaks.

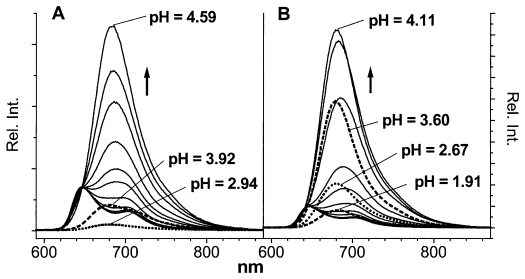

Figure 3. Uncorrected emission spectra of A) $H_2PorphGlu^1OH$ ($N=1$) (**1**), and B) $H_2PorphGlu^2OH$ ($N=2$) (**2**), resulting from excitation at 485 nm. The arrows indicate the directions of the spectral changes occurring upon decrease of pH. Dashed lines show spectra of aggregates.

Table 2. Fluorescence data of $H_2PorphGlu^NOH$ in water solutions.

Generation	Excitation (nm)	Free-base $H_2PorphGlu^NOH$ (λ, nm)	Protonated di-acid $(H_4PorphGlu^NOH)$dendrimer^{2+} (λ, nm)
***N*=1**	485	646, 702	682, 680[a]
***N*=2**	485	647, 703	682, 680[a]
***N*=3**	415	609,[b] 650, 701	–
	440	–	680
	485	652, 703	683, 697[c]

[a] Assigned to the aggregates formed upon acidification. [b] Assigned to the mono-protonated form $(H_3PorphGlu^3OH)^+$. [c] Hypothetical assemblies between dendrimers.

The fluorescence spectra of non-protonated dendrimer–porphyrins have a classical pattern, namely two bands, symmetrical to the corresponding absorptions.[15] The larger band (Q(0,0)) moves almost 5 nm to the red from 646 ($N=1$) to 651 ($N=3$), which is consistent with the trend in the absorption spectra (vide supra). Diprotonation induces the merge of Q(0,0) and Q(1,0) bands, reflecting a D_{2h} to D_{4h} symmetry transition in the core porphyrins. The peak, corresponding to the di-protonated form $(H_4PorphGlu^NOH)^{2+}$, is located at 681–682 nm in all of the compounds in the series ($N=1-3$).

The aggregation caused a substantial decrease in the fluorescence intensity in **1** and **2** after pH reached the values of 4.59 and 4.11, respectively. This decrease was clearly observed despite the fact that the intensity of absorption at the excitation wavelength (485 nm) increased due to the "red migration" of the Soret bands. As a result, the second protonation constant K_4 (Scheme 1) could not be measured for **1** or for **2** without special solubilizing agents.[19b] However, the mono-protonation constant, K_3, could be determined for the entire series of dendrimers using fluorescence rationing. For **1** there was a clear isosbestic point at 630 nm, while the band at 703 nm underwent rapid change with pH in the range of protonation. Therefore, the ratio of emission intensities at these two wavelengths seemed an appropriate indicator for the transition. Figure 4 shows the corresponding plots (I_{630}/I_{703} versus pH) for all three dendrimers.

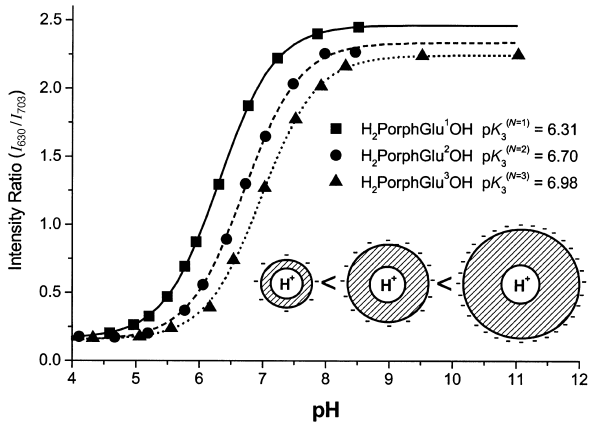

Figure 4. Fluorescence intensity ratios I_{630}/I_{703} versus pH in $H_2PorphGlu^N$-OH ($N=1-3$) series. The emission spectra are obtained from excitation at 485 nm. Lines show analytical fitting of the data to Henderson-Hasselbalch curves with $n=1$, corresponding to the first N-protonation (K_3).

The experimental data were fit to the Henderson–Hasselbalch equation with $n=1$, confirming a single ionization process. It is worth mentioning that for most *meso*-tetraphenylporphyrins, pK_3 and pK_4 cannot be determined separately. The measurements give $(pK_3+pK_4) \approx 5$ and non-integral values for n.[19a, 21] In the series of dendrimer–porphyrins, pK_3 gradually shifts alkaline (0.3–0.4 pH units per generation); this suggests growing stabilization of the central positive charge by the increasing negative charge on the dendrimer periphery. Such a shift in pK_3 is another demonstration of the electrostatic shielding effect, consistent with the reported decrease in redox potentials in the series of dendritic Zn-porphyrins[4a,c].

Additional titrations were performed with the largest dendrimer, **3**, in order to evaluate the second ionization constant K_4. In these experiments the emission was excited at 440 nm [λ_{Soret} of di-protonated form $(H_4PorphGlu^3OH)^{2+}$] and at 418 nm (λ_{Soret} of non-protonated $H_2PorphGlu^3OH$). The resulting spectra as well as the plots of fluorescence intensity versus pH are shown on Figure 5 (A–D).

There is an additional small peak at 609 nm (Figure 5, A) which rises upon acidification, reaches its maximum at pH of about 6.15 and then disappears again. Most likely this emission originated exclusively from mono-protonated por-

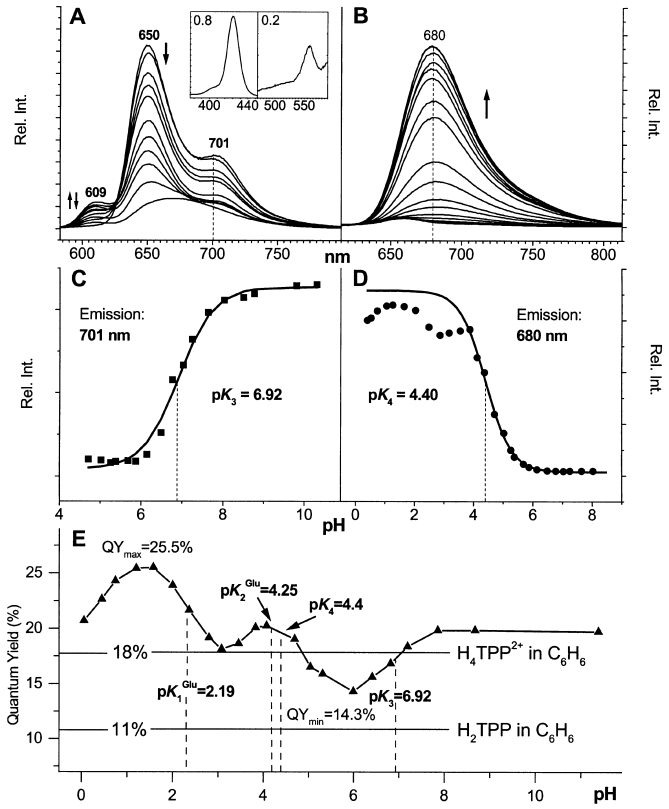

Figure 5. Changes induced by N-protonation in the fluorescence spectra of H_2PorphGlu^{3}OH (N = 3) (**3**). The spectra were obtained using excitation at A) 415 nm (insert shows the corresponding excitation spectrum for the emission at 609 nm, pH 6.17), and B) 440 nm. The arrows indicate the directions of the spectral changes with decrease of pH. The corresponding plots of fluorescence intensity versus pH were measured at C) 701 nm; and D) 680 nm. The solid lines indicate analytical Henderson–Hasselbalch curves ($n = 1$) for the first (K_3) and the second (K_4) porphyrin protonations respectively. E) Fluorescence quantum yield of **3** versus pH. Fluorescence was excited at 425 nm. Vertical dashed lines show pK_as of glutamic acid (2.19 and 4.25) and of the porphyrin protonations (pK_3 = 6.92 and pK_4 = 4.40). Horizontal lines correspond to the quantum yields of H_2TPP in aerated C_6H_6 (11 %)[14] and its di-cation H_4TPP^{2+} (18 %), formed upon acidification with CF_3COOH.

phyrin (H_3PorphGlu^{3}OH)$^+$. This form was later identified by the corresponding excitation spectra (Figure 5, A (insert); $\lambda_{Soret} = 424$ nm, $\lambda_Q = 559$ nm).

The fit of the first set of points ($\lambda_{ex} = 418$ nm, $\lambda_{em} = 701$ nm) with $n = 1$ curve (dashed line) (Figure 5, B) gave p$K_3 = 6.92$ (± 0.05), which was only slightly different from the value obtained in the previous titration (p$K_3 = 6.98 \pm 0.02$). The course of the second protonation ($\lambda_{ex} = 440$ nm, $\lambda_{em} = 680$ nm) (Figure 5, C), in the pH range of 6.2–3.5, could not be followed to completion. However, the distortion of the curve did not begin until pH ≈3.85, and the first several points still could be fit to the Henderson–Hasselbalch equation with $n =$ 1 (dotted line), resulting in a pK_4 value of 4.4 (± 0.03). Hence, the difference between the pKs (pK_3 − pK_4 ≈2.55) was found more than one pH unit larger than typically obtained for *meso*-phenyl substituted porphyrins (1.5 units).[16] We think that this is due to the alkaline shift in the constant K_3, which must be more affected by the dendritic environment around the porphyrin than is K_4. When the first protonation (K_3) occurs, glutamic carboxyls are still ionized and their negative charges result in a partial stabilization of the protonated core-porphyrin. On the other hand, the second protonation (K_4) takes place in the same pH region as the protonation of the peripheral carboxyls.[20] When dendritic branches are protonated (uncharged), they no longer provide an electrostatic shield, leaving the core-porphyrin to behave more like a free, unprotected one.

The plot of the fluorescence intensity (Figure 5 C, D) appeared to be almost completely consistent with the pH dependence of the fluorescence quantum yield (Figure 5, E). The latter was determined in the solutions of **3** and referenced to that of *meso*-tetraphenylporphyrin (H_2TPP) in benzene C_6H_6 (11 %)[14] and its di-cation (H_4TPP^{2+}), produced by the addition of trifluoroacetic acid (18 %). Overall, the quantum yield of **3** was higher than that of both un-protonated and protonated forms of the standard. This is probably due to the less effective fluorescence quenching in water than in C_6H_6 as well as to lower oxygen solubility in water. (Dissolved oxygen was found to reduce porphyrin fluorescence in benzene by about 15 %.)[22] The quantum yield of **3** increased from 19.8 % (pH 8.7) to 25.5 % (pH 1.6) upon acidification. However, in the beginning, as pH is lowered, the quantum yield decreased, following almost exactly the first protonation curve (K_3). The following increase reflects the second protonation (K_4), but at pH ≈4 the quantum yield began to decline and then again rose at pH ≈3. This rising brought the emission up to 25.5 %, its highest value in the set. Starting with pH ≈1.6 there is, however, another steady decline as acidity increases.

Such pH dependence of the quantum yield was found to be highly consistent. It was reproduced using various dilutions of **3** and various excitation wavelengths. However, the interpretation of the pattern would require additional studies, since a number of rather complex phenomena might influence the fluorescence quantum efficiency. These include internal reorganization of dendritic branches as the negative charge, and therefore electrostatic repulsion, decreases with protonation of the peripheral carboxyl groups (pK_as of glutamic acid are shown on Figure 4, E); increased self quenching due to closer contact among chromophors in dendrimer assemblies at a low pH; a different efficiency of the quenching by solvent at varying pH values, etc.

As mentioned above, with an increase in acidity (pH ≈0.01) the absorption bands of **3** shift down to the red (see Figure 2, C). The emission spectra, resulting from excitation at different wavelengths, were recorded for this extra-acidic sample. As expected, the emission bands were asymmetrical, showing a longer wavelength "shoulder", similarly to H_4^{2+}TCPP in 10 % trifluoroacetic acid solutions.[17b] There is a clear shift in the emission maximum of more than 10 nm to the red as the excitation wavelength is changed from 455 to 495 nm (Figure 6). This suggests the presence of longer wavelength-absorbing intermolecular assemblies. The excitation spectra, recorded for emissions at 665, 715, 765, and 815 nm, also show a slight migration of the Soret peak.

The spectroscopically measured pH dependencies described in this paper demonstrate the significant influence of the dendritic polyglutamic environment on properties of the central core. More specifically, variations in the dendrimer

0947-6539/00/0613-2460 $ 17.50+.50/0 *Chem. Eur. J.* **2000**, *6*, No. 13

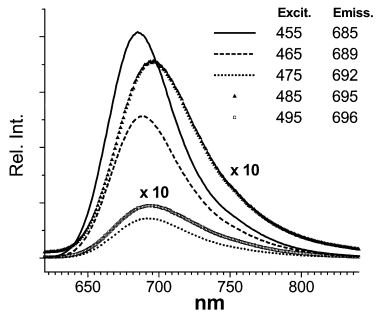

Figure 6. Uncorrected emission spectra of the acidified sample (pH ≈ 0.01) of H_2PorphGlu^{3}OH (N = 3) (**3**) resulted from excitation at different wavelengths. The intensities of the spectra marked with "× **10**" are enlarged by a factor of 10.

size are shown to alter the protonation constants of the encapsulated porphyrin. An important result is that the value of the first protonation constant of the three-layered dendrimer–porphyrin H_2PorphGlu^{3}OH, pK_3 = 6.98, is appropriate for broad pH sensing in biological systems. This combined with almost unlimited water solubility, impermeability through the biological membranes, and the high quantum efficiency of fluorescence make H_2PorphGlu^{3}OH a promising new pH indicator.

Acknowledgement

This work was supported by Grants CA-74062 and HL-60100 from National Institutes of Health (NIH).

[1] a) D. K. Smith, F. Diederich, *Chem. Eur. J.* **1998**, *4*, 1353; b) F. W. Zeng, S. C. Zimmerman, *Chem. Rev.* **1997**, *97*, 1681; c) M. Fischer, F. Vögtle, *Angew. Chem.* **1999**, *111*, 934; *Angew. Chem. Int. Ed. Engl.* **1999**, *38*, 885; d) G. R. Newkome, E. He, C. N. Moorefield, *Chem. Rev.* **1999**, *99*, 1689.

[2] D.-L. Jiang, T. Aida, *Chem. Commun.* **1996**, 1523.

[3] a) R.-H. Jin, T. Aida, S. Inoue, *Chem. Commun.* **1993**, 1260; b) J. P. Collman, L. Fu, A. Zingg, F. Diederich, *Chem. Commun.* **1997**, 193; c) D. L. Jiang, T. Aida, *J. Macromol. Sci. Pure Appl. Chem.* **1997**, *A34*, 2047.

[4] a) P. J. Dandliker, F. Diederich, M. Gross, C. B. Knobler, A. Louati, E. M. Sanford, *Angew. Chem.* **1994**, *106*, 1821; *Angew. Chem. Int. Ed. Engl.* **1994**, *33*, 1739; b) P. J. Dandliker, F. Diederich, J.-P. Gisselbrecht, A. Louati, M. Gross, *Angew. Chem.* **1995**, *107*, 2906; *Angew. Chem. Int. Ed. Engl.* **1995**, *34*, 2725; c) P. J. Dandliker, F. Diederich, A. Zingg, J. P. Gisselbrecht, M. Gross, A. Louati, E. M. Sanford, *Helv. Chim. Acta* **1997**, *80*, 1773.

[5] a) P. Bhyrappa, J. K. Young, J. S. Moore, K. S. Suslick, *J. Am. Chem. Soc.* **1996**, *118*, 5708; b) P. Bhyrappa, G. Vaijayanthimala, K. S. Suslick, *J. Am. Chem. Soc.* **1999**, *121*, 262.

[6] a) Y. Tomoyose, D.-L. Jiang, R.-H. Jin, T. Aida, T. Yamashita, K. Horie, E. Yashima, Y. Okamoto, *Macromol.* **1996**, *29*, 5236; b) N. Tomioka, D. Takasu, T. Takahashi, T. Aida, *Angew. Chem.* **1998**, *110*, 1611; *Angew. Chem. Int. Ed. Engl.* **1998**, *37*, 1531; c) M. Numata, A. Ikeda, C. Fukuhara, S. Shinkai, *Tetrahedron Lett.* **1999**, *40*, 6945.

[7] a) R. Sadamoto, N. Tomioka, T. Aida, *J. Am. Chem. Soc.* **1996**, *118*, 3978; b) K. W. Pollak, J. W. Leon, J. M. J. Fréchet, M. Maskus, H. D. Abruna, *Chem. Mater.* **1998**, *10*, 30.

[8] D. L. Jiang, T. Aida, *J. Am. Chem. Soc.* **1998**, *120*, 10895.

[9] K. W. Pollak, E. M. Sanford, J. M. J. Fréchet, *J. Mater. Chem.* **1998**, *8*, 519.

[10] a) S. A. Vinogradov, D. F. Wilson, *Adv. Exp. Med. Biol.* **1997**, *428*, 657; b) S. A. Vinogradov, L. W. Lo, D. F. Wilson, *Chem. Eur. J.* **1999**, *5*, 1338.

[11] F. Vögtle, M. Plevoets, M. Nieger, G. C. Azzellini, A. Credi, L. De Cola, V. De Marchis, M. Venturi, V. Balzani, *J. Am. Chem. Soc.* **1999**, *121*, 6290.

[12] M. Gouterman in *The Porphyrins*, *Vol. III* (Ed.: D. Dolphin), Academic Press, New York, **1979**, pp. 1–165.

[13] N. Datta-Gupta, T. J. Bardos, *J. Heterocycl. Chem.* **1966**, *3*, 495.

[14] P. G. Seybold, M. Gouterman, *J. Mol. Spectrosc.* **1969**, *31*, 1.

[15] M. Gouterman, *J. Mol. Spectrosc.* **1961**, *6*, 138.

[16] P. Hanbright, in *Porphyrins and Metalloporphyrins* (Ed.: K. M. Smith), Elsevier, Amsterdam, **1975**, pp. 233–278.

[17] a) D. L. Akins, H.-R. Zhu, C. Guo, *J. Phys. Chem.* **1994**, *98*, 3612; b) D. L. Akins, H. R. Zhu, C. Guo, *J. Phys. Chem.* **1996**, *100*, 5420; c) D. L. Akins, S. Ozcelik, H. R. Zhu, C. Guo, *J. Phys. Chem.* **1996**, *100*, 14390.

[18] a) R. F. Khairutdinov, N. Serpone, *J. Phys. Chem. B* **1999**, *103*, 761; b) N. C. Maiti, S. Mazumdar, N. Periasamy, *J. Phys. Chem. B* **1998**, *102*, 1528.

[19] a) R. F. Pasternak, P. R. Huber, P. Boyd, G. Engasser, L. Francesconi, E. Gibbs, P. Fasella, G. Cerio Ventura, L. C. Hinds, *J. Am. Chem. Soc.* **1972**, *94*, 4511; b) D. C. Barber, R. A. Freitag-Beeston, D. G. Whitten, *J. Am. Chem. Soc.* **1991**, *95*, 4074; c) J. M.Ribo, J. Crusats, J. A. Farrera, M. L. Valero, *J. Chem. Soc. Chem. Commun.* **1994**, 681.

[20] The pK_a values for glutamic acid are 2.19 and 4.25 (A. L. Lehninger, *Biochemistry*, 2nd ed., Worth Publishers, New York, **1977**, p. 79).

[21] J. Sutter, P. Hambright, M. Krisnamurthu, P. B. Chock, *Inorg. Chem.* **1974**, *13*, 1974.

[22] D. J. Quimby, F. R. Longo, *J. Am. Chem. Soc.* **1975**, *97*, 5111.

Received: October 21, 1999 [F2101]